Earth Surf. Dynam. Discuss., https://doi.org/10.5194/esurf-2018-36
Manuscript under review for journal Earth Surf. Dynam.
Discussion started: 3 May 2018

Earth Surface Dynamics Discussions
Open Access
EGU

Automatic detection of avalanches using a combined array classification and localization

Matthias Heck[1], Alec van Herwijnen[1], Conny Hammer[2], Manuel Hobiger[2], Jürg Schweizer[1], and Donat Fäh[2]

[1]WSL Institute for Snow and Avalanche Research SLF, Davos
[2]Swiss Seismological Service SED, ETH Zurich, Zurich

Correspondence: Matthias Heck (matthias.heck@slf.ch)

Abstract.

We use a seismic monitoring system to automatically determine the avalanche activity at a remote field site near Davos, Switzerland. By using a recently developed approach based on hidden Markov models (HMMs), a machine learning algorithm, we were able to automatically identify avalanches in continuous seismic data by providing as little as one single training event. Furthermore, we implemented an operational method to provide near real-time classification results. For the 2016-2017 winter period 117 events were automatically identified. False classified events such as airplanes and local earthquakes were filtered using a new approach containing two additional classification steps. In a first step, we implemented a second HMM based classifier at a second array $14\,\mathrm{km}$ away to automatically identify airplanes and earthquakes. By cross-checking the results of both arrays we reduced the amount of false classifications by about $50\,\%$. In a second step, we used multiple signal classifications (MUSIC), an array processing technique to determine the direction of the source. Although avalanche events have a moving source character only small changes of the source direction are common for snow avalanches whereas false classifications had large changes in the source direction and were therefore dismissed. From the 117 initially detected events during the 4 month period we were able to identify 90 false classifications based on these two additional steps. The obtained avalanche activity based on the remaining 27 avalanche events was in line with visual observations performed in the area of Davos.

1 Introduction

During the winter seasons, snow avalanches are a common threat in mountain regions. Avalanche warning services therefore inform the public of the current avalanche danger. To assess the danger level, warning services rely on information about the snowpack, amount of new snow, weather conditions and avalanche activity (McClung and Schaerer, 2006). Whereas the first three parameters can be measured or modeled, avalanche activity data are often hard to obtain, especially during snow storms or at night. Monitoring systems have therefore been developed to estimate the avalanche activity for a certain region.

Snow avalanches, like any other mass movement, generate seismic and infrasound waves (e.g. van Herwijnen and Schweizer, 2011b; Suriñach et al., 2005; Marchetti et al., 2015). Seismic signals of avalanches show some common characteristics, such as

Earth Surf. Dynam. Discuss., https://doi.org/10.5194/esurf-2018-36
Manuscript under review for journal Earth Surf. Dynam.
Discussion started: 3 May 2018

a spindle shaped envelope of the time series (Nishimura and Izumi, 1997) and a typical frequency content between 2 and 30 Hz (Schaerer and Salway, 1980; Suriñach et al., 2001). Several classification approaches were therefore developed to automatically detect avalanches in seismic data. Leprettre et al. (1996) used a fuzzy logic approach to distinguish between different types of signals. Bessason et al. (2007) used a nearest neighbor approach to classify new recorded events. Although they relied on a 10-year database of avalanche events, the identification was rather poor. Rubin et al. (2012) compared 12 machine learning algorithms, 10 of which were able to detect at least $90\,\%$ of all known avalanches, however, at the cost of very high false alarm rates. Hammer et al. (2017) recently used hidden Markov models (HMMs), an advanced machine learning algorithm, to automatically detect large avalanches released during the winter of 1998-1999 in seismic data recorded by a single broadband station maintained by the Swiss Seismological Service (SED). Using this approach, they were able to identify 43 avalanches during a 5-day period within a radius of $30\,\mathrm{km}$ of the station. Heck et al. (2018a) also used the HMM approach to automatically detect avalanches, however, in data recorded during the winter season 2009-2010 by a seismic array consisting of seven less sensitive vertical geophones. They obtained the best results for the automatic detection by combining the classification results of all sensors and requiring a minimal event duration for the detections.

In addition to the automatic detection of avalanches, Lacroix et al. (2012) and Heck et al. (2018b) used seismic array processing techniques to locate the source of the avalanche. Lacroix et al. (2012) implemented a beam-forming approach and were able to assign recorded avalanches to three known avalanche paths. Heck et al. (2018b) compared a beam-forming method with a multiple signal classification (MUSIC) approach (Schmidt, 1986) and obtained better results with the latter and applied this method to avalanches monitored during a two-day period in March 2017. However, they also observed that their seismic array mostly recorded infrasound due to the limited distance between their sensors. Nevertheless, they were able to reconstruct the avalanche path of several recorded events.

In several studies, avalanches were automatically identified in infrasonic data by using localization parameters determined using cross-correlation techniques (Scott et al., 2007; Marchetti et al., 2015; Thüring et al., 2015). By comparing the back-azimuth with the directions of known avalanche paths, possible avalanche events were identified (Marchetti et al., 2015). Thüring et al. (2015) used a similar approach for the automatic detection, but relied on support vector machines (SVM), a machine learning algorithm.

Our aim is to automatically identify avalanches in continuous data recorded during the winter period 2016-2017 using the same machine learning techniques based on hidden Markov models as used by Heck et al. (2018a). To reduce the false alarm rate we first use an additional classification performed at a second array $14\,\mathrm{km}$ away to dismiss events recorded almost simultaneously at both arrays such as earthquakes and airplanes. In a second step, we analyze the median back-azimuth path of the detections using the MUSIC method as performed by Heck et al. (2018b) and dismiss all events with a randomly distributed back-azimuth. We perform the classification and localization of the events with the data recorded at a seismic array located in the Dischma Valley above Davos, Switzerland during the winter season 2017 and combine it with the data obtained at the Wannengrat array.

Earth Surf. Dynam. Discuss., https://doi.org/10.5194/esurf-2018-36
Manuscript under review for journal Earth Surf. Dynam.
Discussion started: 3 May 2018

2 Field site and instrumentation

Prior to the 2016-2017 winter season, we installed two seismic arrays above Davos, Switzerland, similar to the systems described by van Herwijnen and Schweizer (2011a). The first array was deployed at the Dischma field site (yellow square in Figure 1), 14 km away from Davos at the end of a tributary valley (Heck et al., 2018b). The field site is a flat meadow at an elevation of 2000 m a.s.l. surrounded by mountain peaks which rise up to 3000 m. The second array was deployed at the Wannengrat field site above Davos at 2500 m a.s.l. (red square in Figure 1). This field site is surrounded by several avalanche starting zones (van Herwijnen and Schweizer, 2011a).

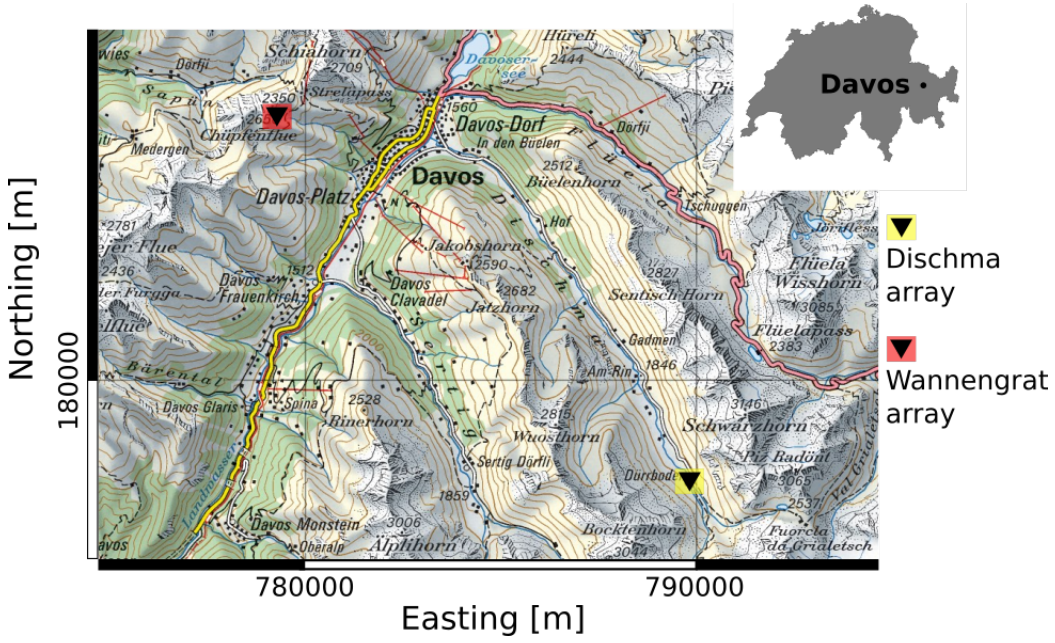

Figure 1. Map of the area of Davos, Switzerland. The two arrays are indicated by a black triangle on colored ground. Red represents the Wannengrat array, yellow the Dischma array. Reproduced by permission of swisstopo (JA100118).

Both arrays consisted of a 300 m long string with 7 vertical component geophones with an eigenfrequency of 4.5 Hz. The sensors of the Dischma array were buried 50 cm deep into the ground whereas the sensors at the Wannengrat field site were attached to rocks using an anchor. For each array the sensors were circularly arranged (Figure 2 a) and b)). The maximum distance between two sensors at the Dischma and Wannengrat field site was 64 m and 74 m, respectively, and the average distance was 36 m at the Dischma array and 45 m at the Wannengrat array.

The instrumentation and data logging systems were identical for both arrays. Data were continuously sampled at a rate of 500 Hz. However, due to technical problems only two sensors of the Wannengrat array recorded data throughout the entire winter (4 and 5 in Figure 2 b)). Both field sites were equipped with several automatic weather stations (3 at Dischma, 4 at Wannengrat) as well as automatic cameras (8 at Dischma, 5 at Wannengrat). The automatic cameras visually monitored the

Earth Surf. Dynam. Discuss., https://doi.org/10.5194/esurf-2018-36
Manuscript under review for journal Earth Surf. Dynam.
Discussion started: 3 May 2018

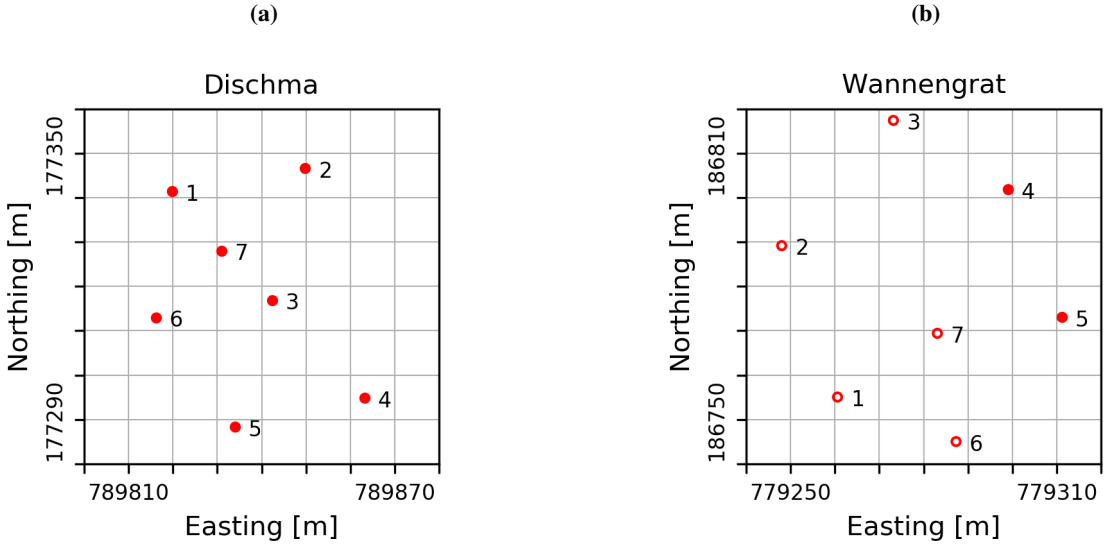

Figure 2. Setup of sensor arrays a) Dischma, b) Wannengrat. The open red circles indicate positions of not working sensors during the winter 2017.

surrounding slopes and images were recorded every 10 minutes throughout the winter. In some cases, these images helped to identify and confirm seismic events produced by avalanches in the data (van Herwijnen and Schweizer, 2011b).

3 Methods

3.1 Data pre-processing

The continuous seismic data mostly consist of noise. Since this noise is of little interest, we applied a simple threshold based event detector to reduce the amount of data (Heck et al., 2018a). For a window i with a length of 1024 samples a mean absolute amplitude A_i was determined. When $A_i \geq 5\overline{A}$, with $\overline{A}$ the daily mean amplitude, the data within the window were processed. Furthermore, a section of $t = 60\,\mathrm{s}$ was cut before and after the window to ensure that the onset and coda of each event was incorporated. In addition, we filtered the data using a 4th order Butterworth bandpass filter with corner frequencies of 1 and $50\,\mathrm{Hz}$.

3.2 Classification of events

To automatically identify avalanches in the continuous seismic data we used hidden Markov models (HMMs). This method was already successfully used on continuous seismic data collected at the Wannengrat field site during the 2009-2010 winter season (Heck et al., 2018a). HMMs are statistical classifiers, which model observations (i.e. the seismic time series or its features) by a sequence of multivariate Gaussian probability distributions. However, the classical approach relying on well known pre-

labeled training sets as performed by Ohrnberger (2001) or Beyreuther et al. (2012) is not suited for the classification of rare seismic events like avalanches. We therefore performed the classification based on a new approach developed by Hammer et al. (2012) exploiting the abundance of data containing mainly background signals to obtain general wave-field properties. Using these properties, a widespread background model can be learned from the general properties. A new event model is obtained by using the background model to adjust the event model description by using only one training event. The so obtained classifier therefore consists of the background model and one model for each interesting event class. The classification process itself calculates the likelihood that an unknown data stream was generated by a specific class for each individual HMM class (Hammer et al., 2012, 2013).

The classification performed by Heck et al. (2018a) consisted of creating a new background model for each day and the resulting HMMs were used to classify the data of the same day. A near real-time classification, as would be required for operational purposes, is then not possible. To overcome this problem, we implemented a classification process by learning the background model using data from a different time window than the data we want to classify. To train the background model we used the pre-processed data taken from the window t_{model}, whereas the pre-processed data we want to classify are in the time window t_{class} (Figure 3). This so-called operational classification was performed by using a window length of $t_{\mathrm{model}} = 24\,\mathrm{h}$ and $t_{\mathrm{class}} = 1\,\mathrm{h}$ with the start time of t_{class} corresponding the end of t_{model}. Once the classification for the window t_{class} is finished, both windows are shifted by one hour. The so performed classification takes $\sim 6\,\mathrm{min}$ for the classification of one day without the feature calculation. In contrast, the classification performed by Heck et al. (2018a) only took $\sim 30\,\mathrm{s}$ for one day. All calculations were performed on a computer with a regularly available 8-core processor and $12\,\mathrm{GB}$ ram running a standard Ubuntu Linux Distribution.

As input for the HMMs a compressed form of the data was used, so-called features. Features represent different aspects of the time series such as spectral, temporal or polarization characteristics. Since we used single component geophones, we only used the following spectral and temporal features similar to those used by Heck et al. (2018a).

- Central frequency
- Dominant frequency
- Instantaneous bandwidth
- Instantaneous frequency
- Cepstral coefficients
- Half-octave bands

For the feature calculation, we used a sliding window of width $w = 512$ samples and a step size of $0.05\,\mathrm{s}$ or 25 samples resulting in an overlap of $97\,\%$. The first half-octave band has a central frequency of $3.9\,\mathrm{Hz}$ and a total number of 6 bands. Calculating the features from the pre-processed data takes $\sim 15\,\mathrm{min}$ for a complete day for all sensors.

Earth Surf. Dynam. Discuss., https://doi.org/10.5194/esurf-2018-36
Manuscript under review for journal Earth Surf. Dynam.
Discussion started: 3 May 2018

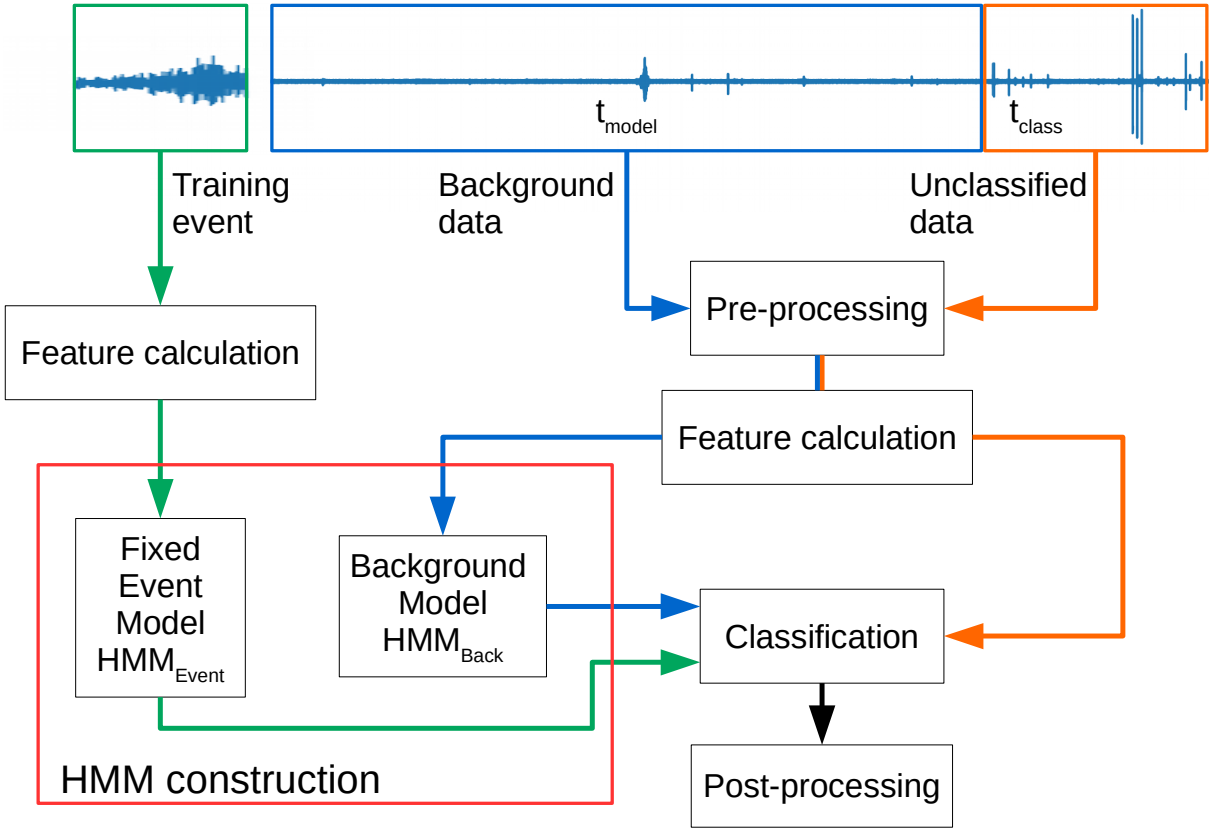

Figure 3. Flow chart of the classification process. Green lines show the construction of the event model. Blue lines show the construction of the background model. The orange lines show, how the data to be classified are processed.

The classification process consists of five steps: pre-processing, feature calculation, HMM construction, classification and post-processing (Figure 3). First the data used to build the background model are selected from the time window t_{model} and the data to be classified are determined by the window t_{class}. The data from the selected time windows are pre-processed to reduce the amount of noise and then the features are calculated. In the HMM construction part, the features calculated from the data within t_{model} and from the data of the training event are used to construct a background model $\mathrm{HMM_{Back}}$ and an event model $\mathrm{HMM_{Event}}$. The event model $\mathrm{HMM_{Event}}$ was determined once and is then applied for the entire winter season. In contrast, the background model $\mathrm{HMM_{Back}}$ was constructed every hour. Using both models, the pre-processed data within the window t_{class} was classified in the classification process. The features calculated for this window are therefore passed to the classifiers. Once the classification is performed, post-processing steps are applied (Heck et al., 2018a). The first step consisted of applying a duration threshold to the classified events. Each classified event having a duration shorter than 12 s was dismissed. The second step, the so-called voting-based classification, combines the results of all sensors. Only events that were classified by at least 5 sensors are considered as possible avalanches.

Earth Surf. Dynam. Discuss., https://doi.org/10.5194/esurf-2018-36
Manuscript under review for journal Earth Surf. Dynam.
Discussion started: 3 May 2018

3.3 Combined array detection

Initial classification results performed on the data set of the winter season 2016-2017 revealed that although the total number of detected events was low, many detected events were very likely generated by airplanes or regional earthquakes (local magnitude between 1.5 and 4 for earthquakes at local and regional distance triggered by at least 6 stations according to the earthquake catalog of the Swiss Seismological Service). In contrast to avalanches, which are recorded only at one array, these events are recorded at both arrays. We therefore used a combined array detection to remove earthquakes and airplanes from the detections. To perform the combined array detection, a second HMM was implemented to identify earthquakes and airplanes in the data recorded at the Wannengrat array $12\,\mathrm{km}$ away from the Dischma array. Classification results were then combined to remove all events recorded simultaneously at both arrays.

3.4 Localization as avalanche indicator

Heck et al. (2018b) determined the direction of several avalanches using a multiple signal classification algorithm called MUSIC and were able to locate the avalanche path of several avalanche events based on the data of a single array. The MUSIC algorithm determines the back-azimuth angle and the apparent velocity of the incoming wave-field for a small time window. This time window is shifted to provide a time series of back-azimuth and apparent velocity values. The MUSIC method is based on the covariance matrix taking the data of all sensors into account at once, whereas beam-forming methods rely on pair-wise cross-correlation (Schmidt, 1986; Rost and Thomas, 2002). MUSIC can resolve multiple sources more easily than beam-forming methods. Furthermore, the MUSIC method can be applied to small frequency bands and the different frequency contents of the wave-field can be analyzed. For further information on multiple signal classification the reader is referred to Schmidt (1986) and Hobiger et al. (2016).

Heck et al. (2018b) found, that due to the small distance between the sensors, the seismic array mostly resolved sonic wave-fields rather than seismic wave-fields to estimate the back-azimuth. Using a median smoothing filter they then calculated a so-called median back-azimuth path with time. In this study, we used these median back-azimuth paths obtained by the event localization to decide whether a classification was a correct or a false alarm. Specifically, we used a threshold value for the derivative of the median back-azimuth path. The assumption is that avalanche events have a smooth median back-azimuth path with little variations, whereas false detections have randomly distributed back-azimuths with large variations in time. By analyzing several avalanche events, especially the events observed by Heck et al. (2018b), we observed small changes below 10° for the back-azimuth path. Even for events passing close to the array we observed small changes below 10° in the median back-azimuth path. Hence, we used a threshold value of 10° between two adjacent points of the median back-azimuth path for the event detection. Similar to the minimum event duration used in the post-processing steps, we require a minimum duration of $20\,\mathrm{s}$ for the back-azimuth path. The minimum duration for this post-processing step is higher than for the minimal duration due to the windowing of $8\,\mathrm{s}$ of the data to obtain the median back-azimuth path (Heck et al., 2018b). They also showed that only the frequency content of the signal between 4.5 and $12.5\,\mathrm{Hz}$ contained information valuable for the localization performed at the used array. By further analysis of the already localized events by Heck et al. (2018b), we observed, that a reduced frequency

range provided similar results. Hence we reduced the number of analyzed frequency bands to 4 bands between 6 and 7.5 Hz and were able to speed up the calculation time. Nevertheless, the processing time for the localization is about three times real time.

4 Classification results

We performed the avalanche detection for the data recorded at the Dischma array during the winter season 2016-2017 and compared the results with the avalanche activity which was visually obtained by local observers and compiled by the avalanche warning service at the SLF. It has to be noted that this compilation is incomplete and covers an area that can not be completely monitored with the Dischma array. Therefore, comparison with this compilation remains indicative.

4.1 Overview of the winter season

The winter period of 2016-2017 was relatively short and characterized by a below-average snow depth. First snowfalls were quite late in the season, in the middle of December, followed by four weeks without substantial precipitation and low temperatures. Due to the constant high temperature gradient within the snowpack, a poorly bonded layer of depth hoar was formed at the base of the snow cover.

During the winter season, three significant snowfall periods were observed; one in each month from January to March (increase of blue line in Figure 4). Each of these snowfalls were associated with considerable avalanche activity in the region of Davos (red bars in Figure 4).

In addition to these avalanche observations, we analyzed the pictures taken by the automatic cameras installed at our field sites. Surprisingly, the avalanche activity was low at the Dischma field site in January and February. During the early March snow storm the visibility was poor and only very few avalanches were identified on the images of the automatic camera. Once the storm was over, the intensity of the avalanche cycle became clear as many avalanche deposits were visible on the images. Five days after the storm we mapped 24 avalanches within a 4 km radius of the Dischma field site (Heck et al., 2018b).

4.2 Classification performed at single array

The main classification was performed at the Dischma field site for all seven sensors. Based on the visual inspection of the seismic data performed by Heck et al. (2018b), several avalanche events suitable as training events for the HMM were identified. However, they had mainly analyzed the period of high avalanche activity on 9 and 10 March 2017. Visually inspecting the entire winter season we identified 44 avalanche events. However, as already shown by Heck et al. (2018a), visually inspecting seismic data also implicates uncertainties. An avalanche released on 9 March 2017 at 06:47 was already analyzed in detail by Heck et al. (2018b) and can unambiguously be classified as an avalanche. We therefore decided to use this event as our training event (Figure 5).

Earth Surf. Dynam. Discuss., https://doi.org/10.5194/esurf-2018-36
Manuscript under review for journal Earth Surf. Dynam.
Discussion started: 3 May 2018

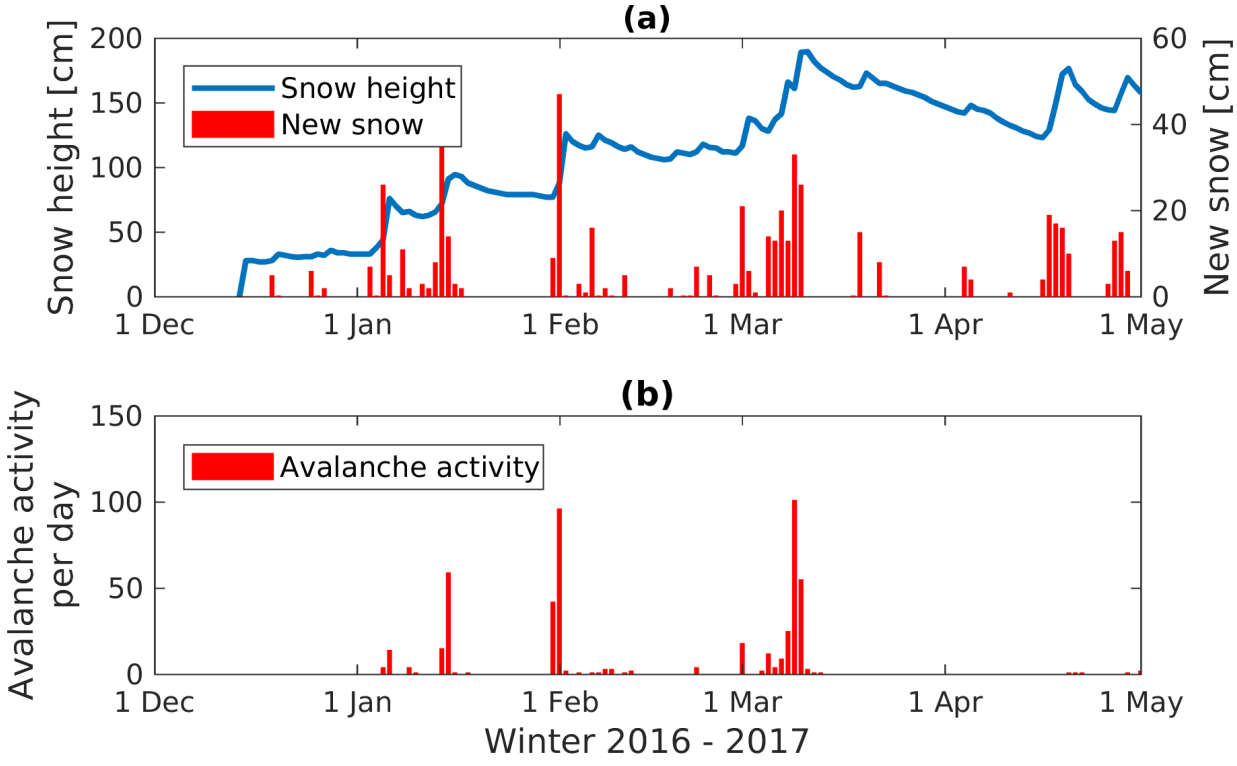

Figure 4. a) Snow height measured at the automatic weather station at Weissfluhjoch $12\,\mathrm{km}$ to the northwest of the Dischma array at $\sim 2600\,\mathrm{m}$ a.s.l. for the winter season 2016-2017. Red bars are the height of new snow measured each day at 8:00 am. b) Number of avalanches observed per day in the region of Davos ($\sim 175\,\mathrm{km}^2$).

Using the classifier trained with this event, we performed the classification for each single sensor of the array. In a next step, the results of the classification were post-processed; first all results of each sensor with a duration $\leq 12\,\mathrm{s}$ were dismissed (Heck et al., 2018a). Finally we dismissed all classifications which were classified by less than 5 sensors.

The classification and the following post-processing was applied to the continuous data set recorded from 1 January to 30 April 2017. For this period, a total of 117 events were classified as avalanches. Half of the events were detected by 7 sensors whereas the classes with 5 and 6 votes are each represented with $25\,\%$ of the events. Most events were classified during the early March snow storm on 9 and 10 March 2017 (Figure 6). In addition a peak in the middle of January and beginning of April as well as a cluster of events around the beginning of February are visible. The peak in January as well as the cluster around the beginning of February correspond with the avalanche activity period visually recorded in the region of Davos (Figure 4). For the peak in April, however, no avalanches were observed in the surroundings of Davos. Furthermore, several single detections are randomly distributed over the season showing no accordance with the visual avalanche observations. Therefore we visually

Earth Surf. Dynam. Discuss., https://doi.org/10.5194/esurf-2018-36
Manuscript under review for journal Earth Surf. Dynam.
Discussion started: 3 May 2018

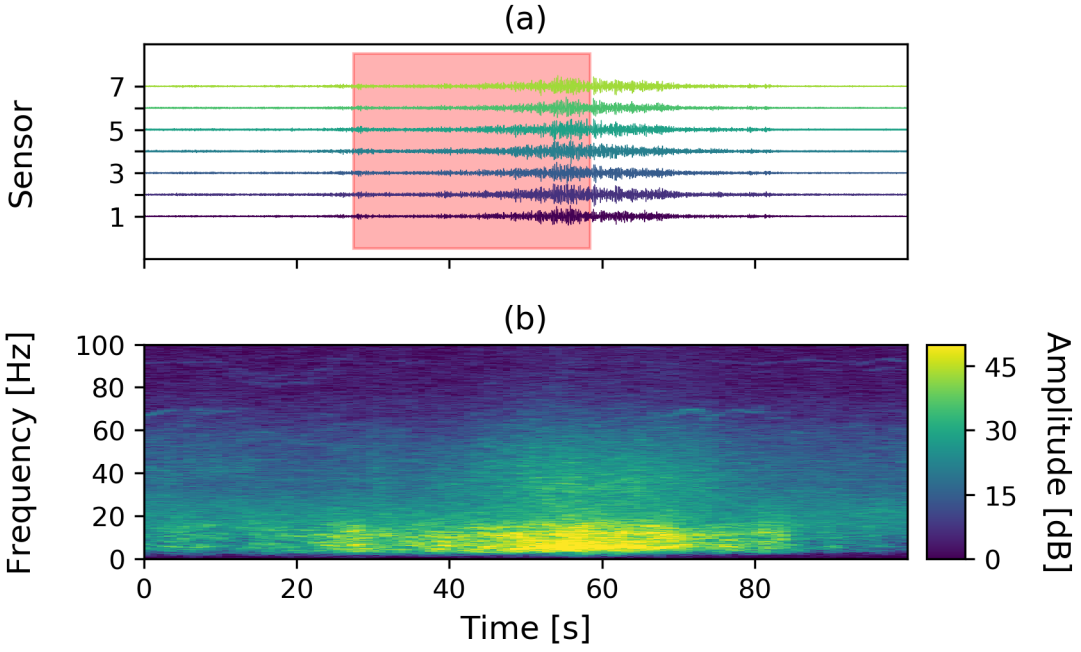

Figure 5. Avalanche released on 9 March 2017 at 06:47 used as training event for the classifier. a) time series for the 7 sensors and b) the corresponding spectrogram. The red area indicates the part of the time series used as training event.

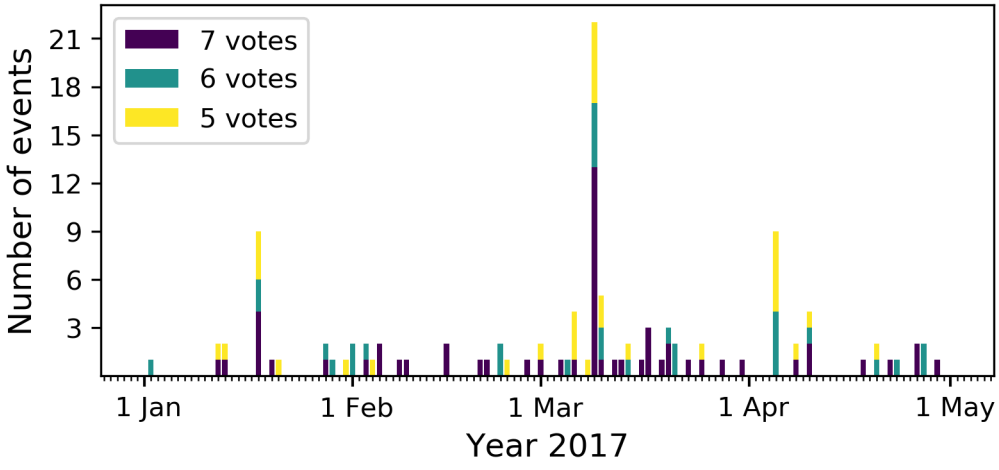

Figure 6. Classification results after post-processing (including voting-based classification) at the Dischma array. The colored bars indicate the number of classified events per day depending on the number of sensors: Violet bar indicates detections by 7 sensor, turquoise bars by 6 sensors and yellow bars by 5 sensors.

Earth Surf. Dynam. Discuss., https://doi.org/10.5194/esurf-2018-36
Manuscript under review for journal Earth Surf. Dynam.
Discussion started: 3 May 2018

inspected the time series and the corresponding spectrograms of each of the 117 classifications and found that the HMM also classified various airplanes (Figure 7 a)) and regional earthquakes (Figure 7 b)) as avalanches.

Although these events can be distinguished from avalanches through visual inspection (e.g. the sharp onset visible for earthquakes), the classifier identified these events as belonging to the avalanche class, even when we used different training events or varied the setup for the classification (results not shown). This was most likely because earthquake and airplane signals were more similar to avalanches than to the background model, and consequently tagged as avalanches.

Analyzing the features also showed the similarities of the different types of events, especially the time dependent behavior. In the beginning of the event, the feature behavior of the events is different, however, at the end of the event a similar time dependent behavior is visible (Figure 8). Due to theses similarities, airplane and earthquake events are more similar to avalanches than to noise resulting in false classifications of these events.

4.3 Classification performed at both arrays

The majority of the misclassifications were produced by two types of events, i.e. airplanes and earthquakes. A comparison of several detected earthquake events with the earthquake catalog of the Swiss Seismological Service (SED) showed, that all compared earthquake events occurred within a range of $120\,\mathrm{km}$. As the Wannengrat array was deployed only $14\,\mathrm{km}$ away, all observed earthquakes were likely to be detected simultaneously at both arrays. Moreover, Davos lies within an approaching corridor of the international airport Zürich and several commercial airplanes are passing by per hour at an altitude of at least $5\,\mathrm{km}$. Similar to avalanches, airplanes also have a moving source character and due to the fast movement they are also observed almost simultaneously at both arrays. Indeed, a comparison of both time series revealed that earthquakes were recorded at both arrays at the same time whereas airplanes were recorded with a small delay of 20 to $30\,\mathrm{s}$ due to the movement of the source. The time series and spectrograms at Dischma and Wannengrat were very similar (Figure 9).

Avalanche signals, however, were only detected within a radius of 3 to $4\,\mathrm{km}$ of the array and were therefore only recorded at one array (Heck et al., 2018b). In order to eliminate classified events recorded at both arrays, we performed a second classification at the Wannengrat array. Due to similarities of the transient signals as mentioned earlier, a HMM trained with an airplane signal was capable to also detect earthquakes. A closer look at the classification results for the Wannengrat array revealed, that it was sufficient to only use the HMM trained with an airplane signal (not shown here). The number of detected events at this array varies strongly per day (blue bars in Figure 10).

The start times obtained by the secondary classification performed with the Wannengrat data were then compared with the classification results for the Dischma array. Overall, 53 of the 117 classifications were detected almost simultaneously at both arrays and we considered theses events as airplanes or earthquakes (yellow bars in Figure 10). After the comparison of the classification results obtained by both arrays 64 potential avalanche events remained (turquoise bars in Figure 10). The distribution of these events is similar to visually observed avalanches (Figure 4), except for detections at the beginning of April. These events were only detected using the automatic classification approach. Furthermore, due to the previously mentioned acquisition problem of the Wannengrat array, all events between 12 and 20 January 2017 were considered as avalanches as

Earth Surf. Dynam. Discuss., https://doi.org/10.5194/esurf-2018-36
Manuscript under review for journal Earth Surf. Dynam.
Discussion started: 3 May 2018

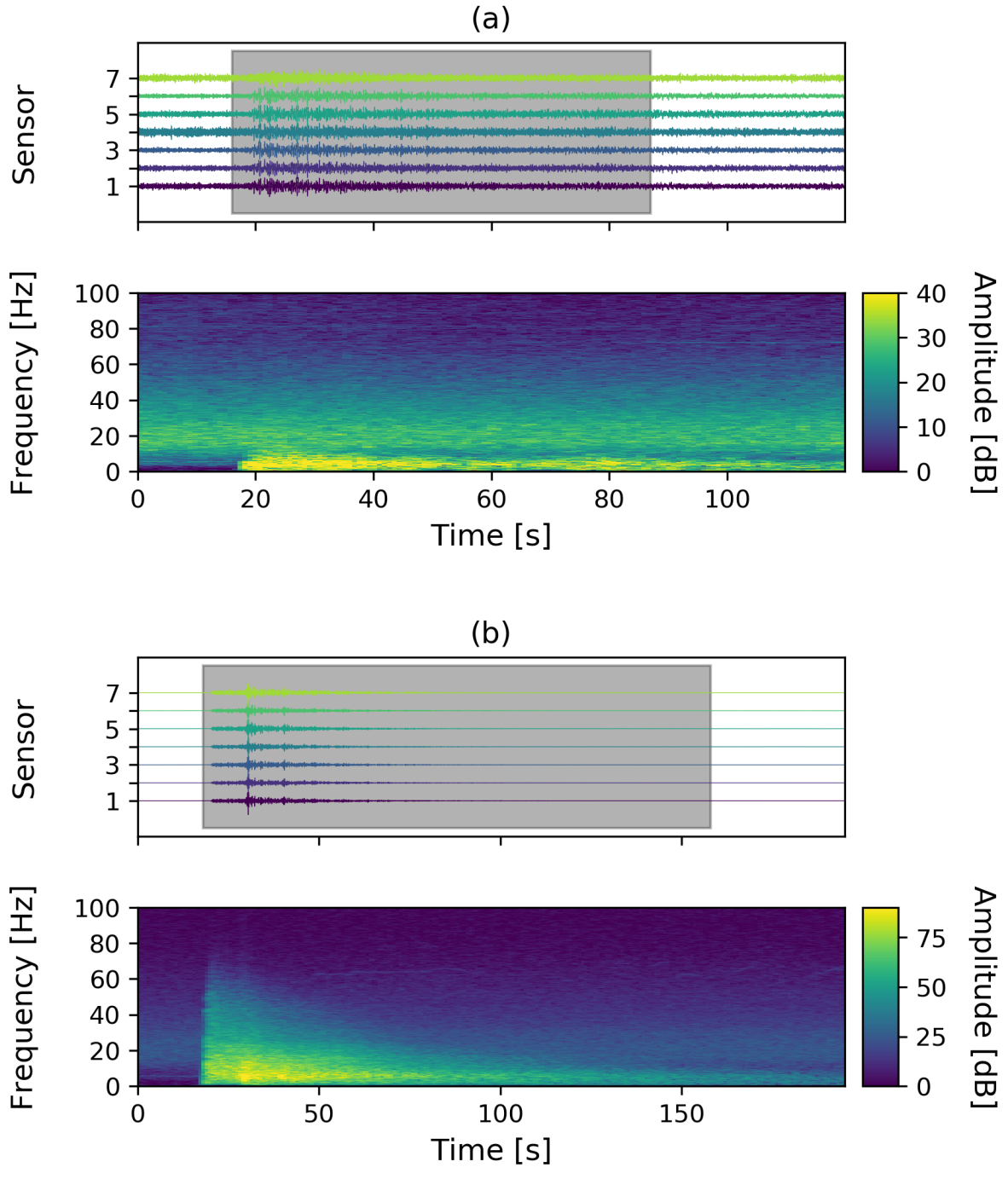

Figure 7. Time series and corresponding spectrograms for two false classifications, a) airplane, b) earthquake. The gray rectangular area indicates the part classified as event by the HMMs.

Earth Surf. Dynam. Discuss., https://doi.org/10.5194/esurf-2018-36
Manuscript under review for journal Earth Surf. Dynam.
Discussion started: 3 May 2018

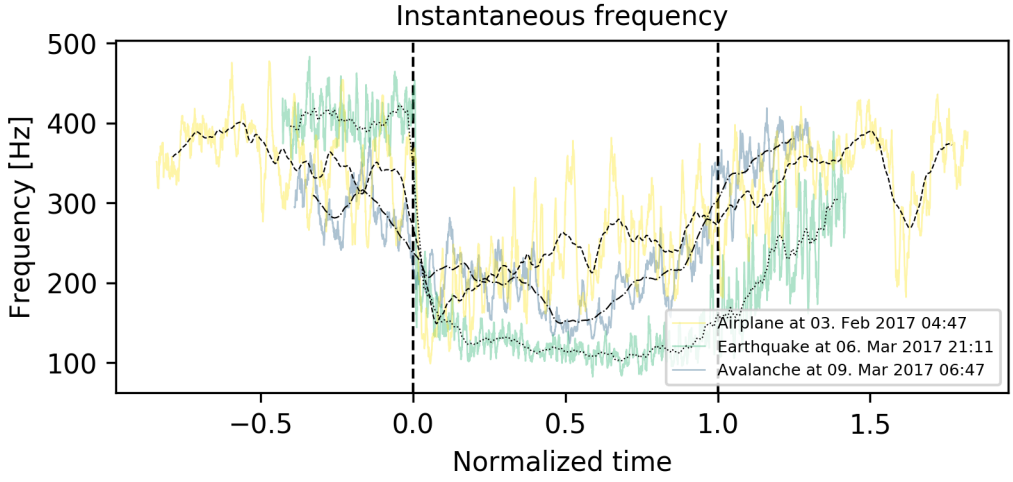

Figure 8. Feature instantaneous frequency for three different event types, yellow represents the signal produced by an airplane, green of an earthquake and blue of an avalanche. The black lines are the mean of the features. The dashed line at 0 indicates the start of the events and the dashed line at 1 the end of the event.

we had no further information from the second array. Hence, we expected some misclassifications among the remaining 64 avalanche events.

4.4 Localization post-processing

In a last processing step, we applied the MUSIC method to the remaining 64 classified events to estimate the back-azimuth and to find a possible median back-azimuth path. The event used to train the HMMs had a duration of around $50\,\mathrm{s}$ showing a median back-azimuth path with slight changes in the angle (straight black line in Figure 11 a)). Before and after the event, however, the back-azimuths were randomly distributed as would be expected for noise. For the training event, the derivative of the back-azimuth path has low values for the $50\,\mathrm{s}$ part with a median back-azimuth path with small changes (Figure 11 b)). For this $50\,\mathrm{s}$ long interval, changes below 10° were observed for the median back-azimuth path. Before and after the event, however, the changes are very high due to the randomly distributed back-azimuths. Further analyzed avalanche events also had changes of the back-azimuth below 10° and we therefore set the 10° as a maximum threshold value. Doing so, another 37 events were dismissed and only 27 avalanche events remained. 15 of the remaining avalanche events were observed during the 9 and 10 March 2017 and some events were detected during the other periods of considerable avalanche activity in February (Figure 4). Furthermore, another 10 single events were also confirmed, but were randomly distributed over the season. For each of the 27 events we determined a mean back-azimuth, which is the mean direction the signals were coming from. The mean back-azimuths were all pointing towards the surrounding slopes where we expected avalanches to release (Figure 13). Events with a duration longer than $100\,\mathrm{s}$ were detected coming either from the north-west or south-east.

Earth Surf. Dynam. Discuss., https://doi.org/10.5194/esurf-2018-36
Manuscript under review for journal Earth Surf. Dynam.
Discussion started: 3 May 2018

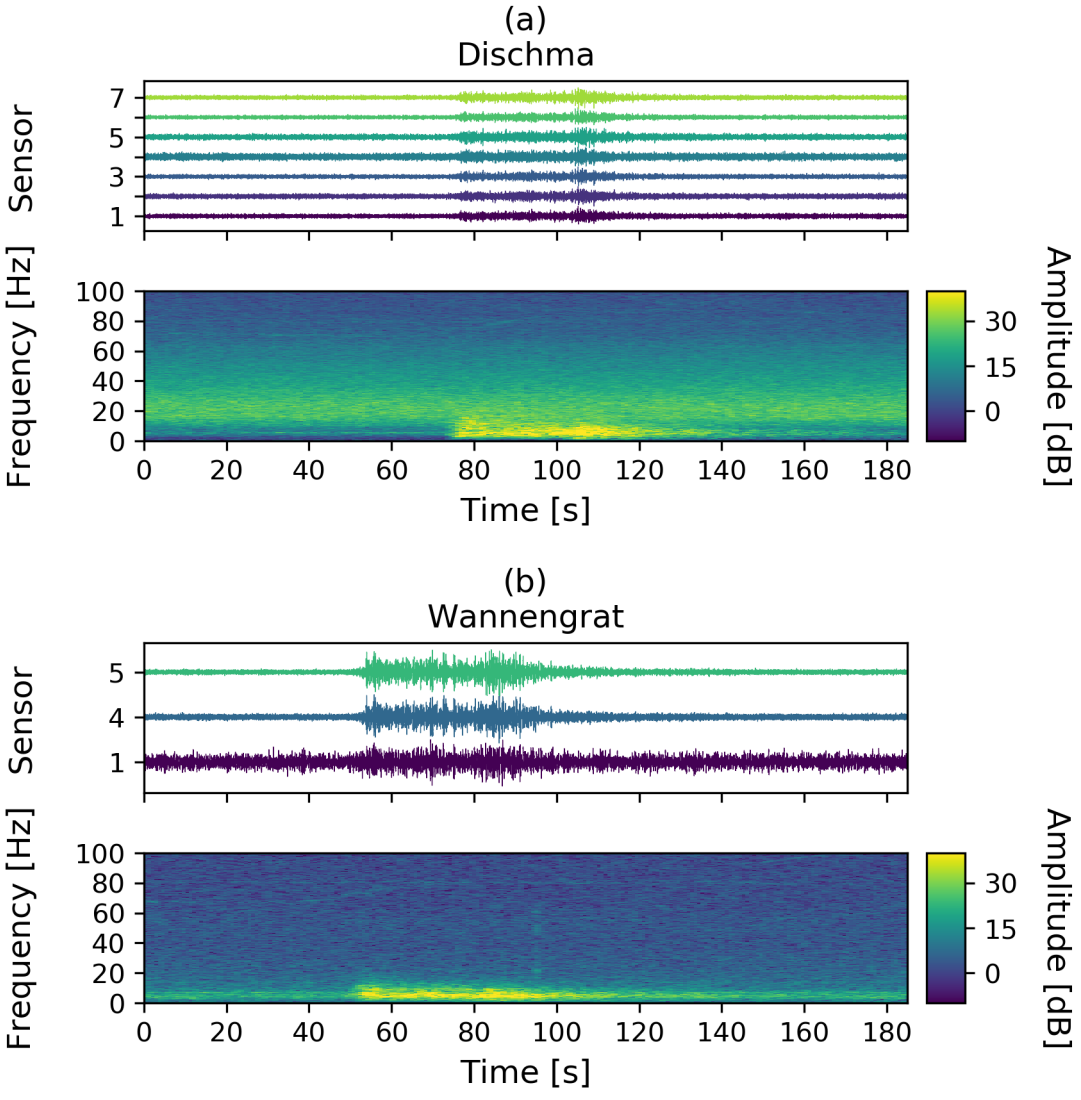

Figure 9. Time series and corresponding spectrograms of an airplane detected at both arrays on 28 January 2017 at 9:17. a) shows the signal recorded at the Dischma array and b) at the Wannengrat array.

Earth Surf. Dynam. Discuss., https://doi.org/10.5194/esurf-2018-36
Manuscript under review for journal Earth Surf. Dynam.
Discussion started: 3 May 2018

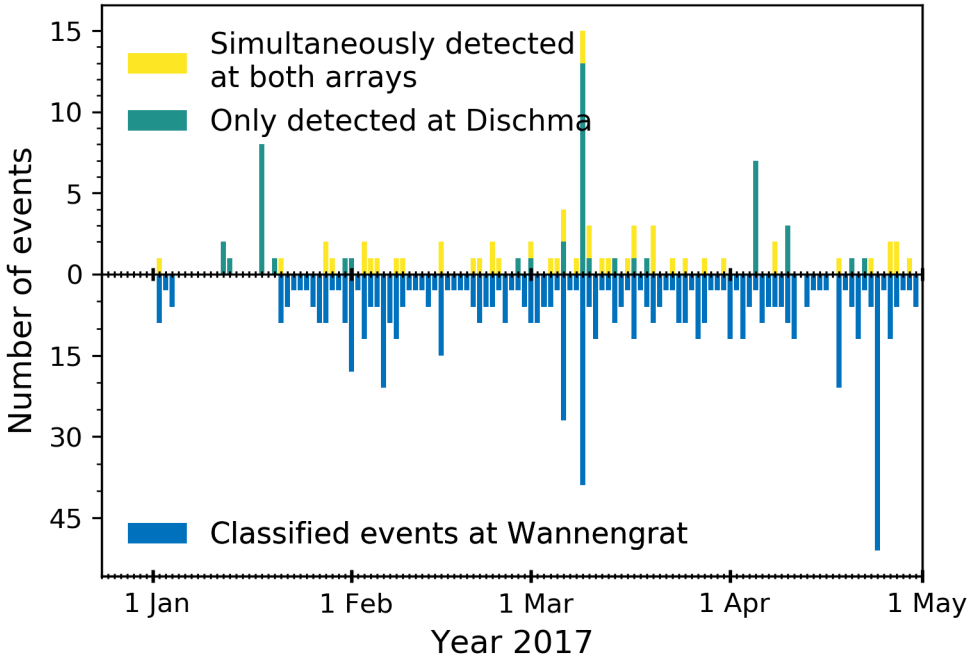

Figure 10. Yellow bars indicate the number of events detected at both arrays and turquoise bars only events recorded at the Dischma array. Blue bars are the number of airplanes and earthquakes detected at the Wannengrat array. Between 5 and 20 January no data were recorded at the Wannengrat array due to technical issues.

Apart from analyzing only the events remaining after the combined array classification, we also performed the localization post-processing for those 53 events we had dismissed. Based on the localization, 48 events were again dismissed, but 5 had a median back-azimuth path within the threshold value. Hence, by directly applying the localization step 32 avalanche events remained, but including at least 5 false detections (15 %).

5 Discussion

We used hidden Markov models (HMMs), a machine learning algorithm, to automatically detect avalanches in data from seismic systems deployed above Davos, Switzerland. The approach builds on the work of Heck et al. (2018a), who adapted the HMM method developed by Hammer et al. (2017) to detect avalanches in continuous seismic data from a small aperture geophone array. Using their approach on our data resulted in automatic detections that still contained a large number of falsely classified events because only one event type (avalanche) and the background noise was used for the classification with HMM.

Earth Surf. Dynam. Discuss., https://doi.org/10.5194/esurf-2018-36
Manuscript under review for journal Earth Surf. Dynam.
Discussion started: 3 May 2018

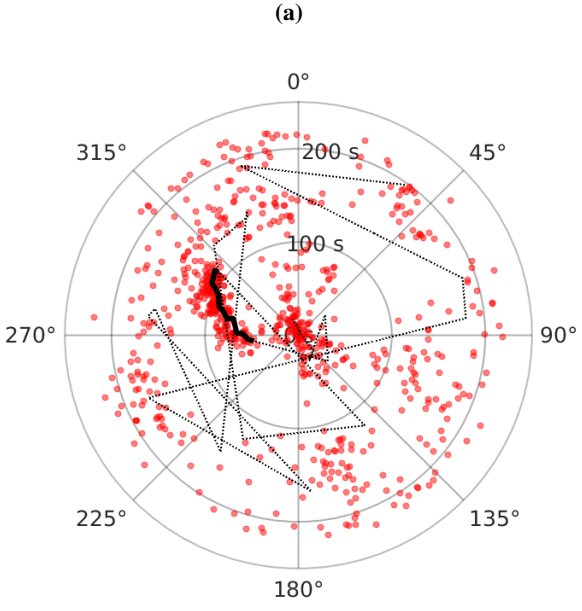

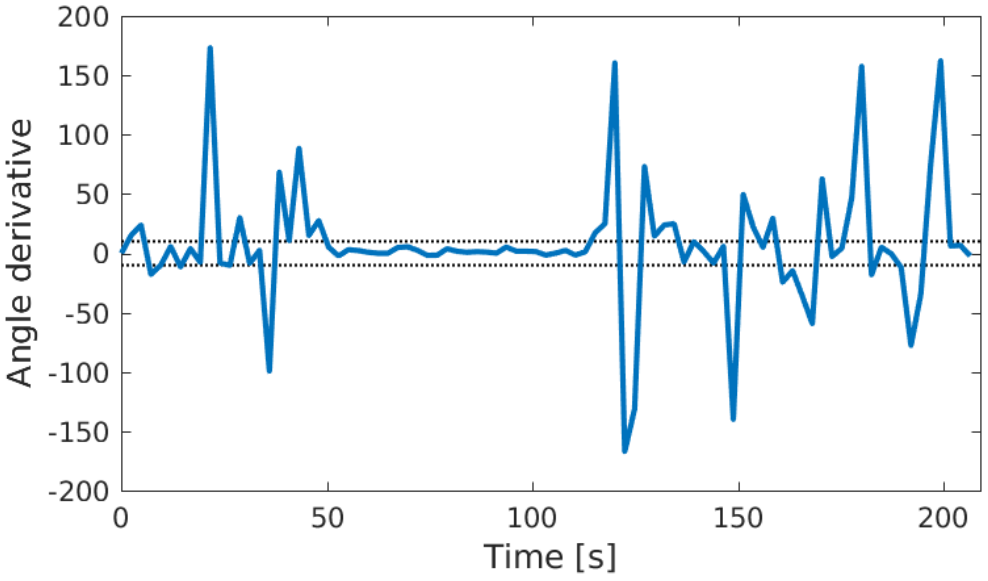

Figure 11. Localization results for avalanche event recorded 9 March 2017 at 6:47 a) polar plot representation of the back-azimuth calculated using the MUSIC method. Red dots are the back-azimuth values for a single time window. The black line represents the median back-azimuth path. The solid part has variations below the threshold whereas the dotted shows strong variations. b) derivative of median back-azimuth path. The dotted lines represents the threshold value of 10°.

Earth Surf. Dynam. Discuss., https://doi.org/10.5194/esurf-2018-36
Manuscript under review for journal Earth Surf. Dynam.
Discussion started: 3 May 2018

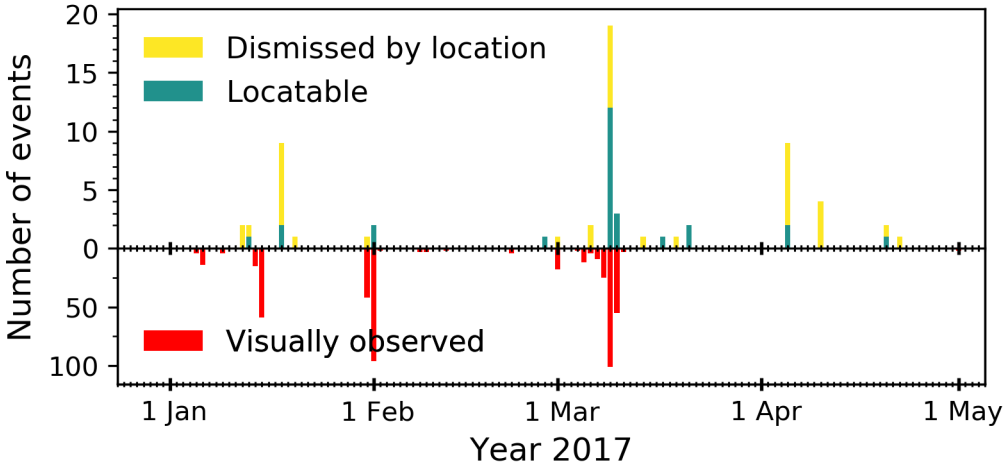

Figure 12. Turquoise bars are the number of events per day which are locatable and are considered as avalanches. Yellow bars are the number of events per day which were not locatable and therefore dismissed. Red bars are the number of avalanches visually observed in the area of Davos.

Earthquake and airplane signals have characteristics closer the avalanches than the background noise, and were therefore included in the detections.

By combining the classification results with a classification performed at a second array located $14\,\mathrm{km}$ away, simultaneously recorded events such as local earthquakes and airplanes could be dismissed. In addition, we applied the multiple signal classification (MUSIC) method to estimate the back-azimuth of the detected events to eliminate false alarms. Overall, this work flow allowed us to automatically identify 27 events that were very likely generated by avalanches, as the temporal trend corresponded well with the avalanche activity for the region of Davos obtained through conventional visual field observations (Figure 4 and 12). It was not possible to confirm any event with visual observations since most avalanches released during periods of bad visibility. However, based on the work of Heck et al. (2018b), we were able to confirm another 12 events identified during 9 and 10 March 2017.

Recent work with HMMs by Heck et al. (2018a) highlighted the difficulty in obtaining a reliable classifier trained on data from a geophone array very similar to the one used in this work. Their results showed that there were large differences in model performance between the sensors, with the number of detections per sensor ranging from about 150 to over 2000. This was attributed to local heterogeneities as the sensors were packed in a Styrofoam housing and inserted within the snowpack. Heck et al. (2018a) therefore suggested to deploy the sensors below the snow cover and either on or below the ground. In our deployment, the geophones were buried about half a meter below the ground on a flat meadow. This approach was successful as it resulted in a much more consistent number of detections per sensor, ranging from 125 to 169. Clearly, the deployment strategy can have a substantial influence on the performance of the classifier.

Earth Surf. Dynam. Discuss., https://doi.org/10.5194/esurf-2018-36
Manuscript under review for journal Earth Surf. Dynam.
Discussion started: 3 May 2018

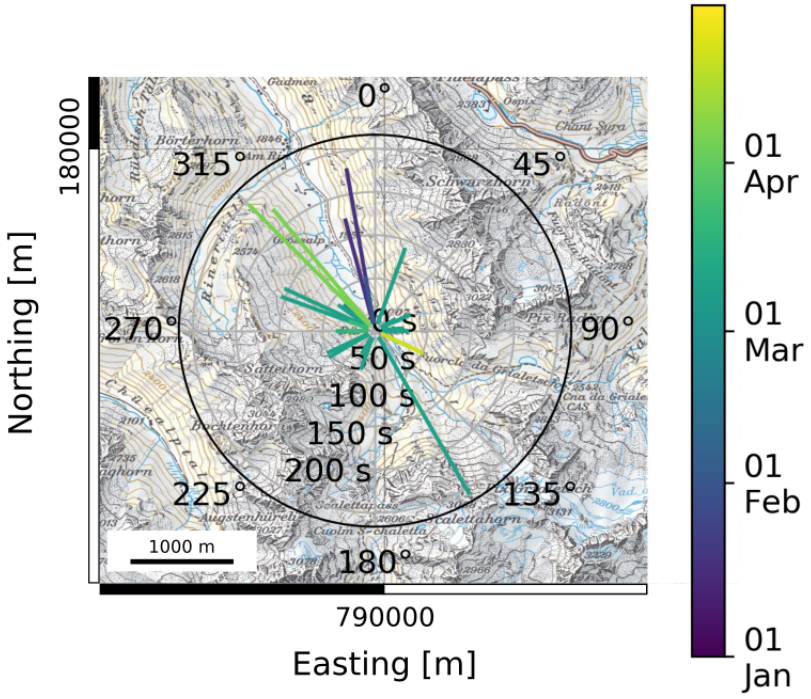

Figure 13. Polar plot representation overlaid on a map section of the field site. The radius indicates the duration of the event, the angle represents the direction of the origin of the event. The different colors of the lines represent the time of the year. Reproduced by permission of swisstopo (JA100118).

In contrast to the classification approach used by Hammer et al. (2017), who were able to use a fixed background model as they analyzed a relatively short period (5 days), we used an approach more suited for operational purposes. Indeed, for the operational set-up the background model was determined using 24 hours of data prior to the hourly data that were classified. In combination with the post-processing steps related to signal duration and number of votes suggested by Heck et al. (2018a), the HMMs identified 117 possible avalanche events (Figure 6). Even though this approach identified the main avalanche cycle in March 2017 (compare Figure 4 and Figure 6), visual inspection of the classified events indicated that at least 50 % of the events were false alarms produced by distant airplanes or regional earthquakes (Figure 7). Even by training a classifier with different feature combinations, changing the training event and/or the length of the training event, the classification results did not substantially change and airplanes and earthquakes were still classified as avalanches. This highlights the difficulty in training an accurate HMM for low energy signals generated by avalanches. We concluded that using HMMs to automatically identify avalanches in seismic data from our geophone array will inherently contain false detections, as the overall feature behavior from distant airplanes or regional earthquakes were very similar to signals generated by avalanches (Figure 8).

Earth Surf. Dynam. Discuss., https://doi.org/10.5194/esurf-2018-36
Manuscript under review for journal Earth Surf. Dynam.
Discussion started: 3 May 2018

To circumvent the problem of developing an optimal event classifier for one specific array, we made use of a second array at the Wannengrat. There we performed a second classification to automatically identify airplanes and earthquakes using an event model trained by an airplane event. Since transient signals produced by earthquakes, airplanes or avalanches have similarities, the results obtained for the second classification based on the airplane event model also falsely identified avalanches and earthquakes. Hence, a classification performed with only one event model was sufficient. The assumption for the second classification was that most falsely classified events were recorded at both arrays. Comparing the time series of detected events at both arrays allowed us to dismiss about $50\,\%$ of the classified events (Figure 10). Identifying co-detections across arrays is therefore an efficient approach to reduce the number of false alarms. Although it was possible, that the classification results of the second array contained avalanche events, it was really unlikely that two avalanches released simultaneously at both field sites. Furthermore, avalanches were only recorded at one array since distance between both arrays was about $14\,\mathrm{km}$. In the future, a promising approach could be to reduce the distance to about 2 or 3 km, as this could also help improving the localization, while still allowing to dismiss false alarms.

Although the combination of two arrays for the classification allowed us to reduce the number of false classification, some uncertainty remained about the origin of the identified events. In a final step, we therefore used the MUSIC method to estimate the median back-azimuth path, as suggested by Heck et al. (2018b), to further dismiss false detections. Similar approaches were suggested for the automatic detection of avalanches in infrasonic data by Marchetti et al. (2015) and Thüring et al. (2015). In those studies, the back-azimuth of continuous infrasound data was calculated on the fly using cross-correlation techniques, and only events with slight changes in back-azimuth over a predefined minimal duration were assumed as avalanche events. In contrast, here we only determined the back-azimuth for events automatically identified by the HMM with the MUSIC method, as Heck et al. (2018b) showed that for our instrumentation pair-wise cross-correlation technique (beam forming) did not result in robust back-azimuth estimates. This last processing step further reduced the number of classified events to 27 (Figure 12). We also found out, that the MUSIC method would have been sufficient to determine the reliability of a detection as it was not possible to locate airplane or earthquake events with our array. After applying the localization based step to all detections, 32 events were identified as avalanches, 5 more events compared to the combined array and the localization based classification.

After applying the combined array classification and the MUSIC method to the data, 27 classification remained for the winter season 2017. Nearly all of theses classifications occurred during periods of observed high avalanche activity (Figure 12). However, for the first two periods of high avalanche activity in January and February only few events were detected, whereas in the surroundings of Davos many events were observed. This may be due to fact that the Dischma site is located about $12\,\mathrm{km}$ to the southeast of Davos and weather and snow conditions are sometimes different since major storms arrive form the northwest. Indeed, based on the images from the automatic cameras, very little avalanche activity was observed in the area in January and February. Nevertheless, it was possible to reconstruct the avalanche activity period in March based on the automatic classification. Results from the localization showed that during the season avalanches released from many different slopes at the field site (Figure 13). This could be observed especially during the snow storm in March. A seismic monitoring system is therefore a suitable tool to monitor a wide area and not just one single slope. Although the detection range is with 3 -

4 km rather small (Heck et al., 2018b) the seismic system in combination with an automatic classifier provides great potential to identify the major avalanche periods.

Based on the here presented approach, a near real-time classification of the seismic data and hence a near real-time detection of avalanches seems possible. The computational times on a computer with a regularly available 8-core processor with 12 GB ram are reasonably short and almost near real-time whereas the localization based on the MUSIC is very costly (three times real time). Although we decided to implement a combined array classification step to save computational time, directly localizing every detection is also possible. Since the amount of detections for the whole season was very low, a near real-time detection could be provided with or without the combined array classification. In future systems, pre-processing steps can be integrated in the data logging unit to reduce the amount of data while recording. Using a standard personal computer, feature calculation is performed near real-time for all sensors simultaneously as well as the HMM construction and the classification. However, a major obstacle of our method is the necessity of an adequate training event recorded at the seismic array. Using training events recorded at different arrays will not work due to possible differences in the instrumentation and changes in the overall background noise or local heterogeneities in the local geology and in snow conditions. To set up the classification experts will be still needed to define correct and confirmed training events. Future research will check the possibility to use one training event for several seasons recorded at the same array.

6 Conclusions

During the winter season 2016-2017 we used a seismic array to continuously monitor avalanche activity in a remote area above Davos, Switzerland. By implementing an operational classification method based on hidden Markov models (HMMs), we were able to detect 117 events in the seismic data from January to April, which were likely produced by avalanches. Subsequent visual inspection revealed a false alarm rate of at least 50 %. Most of the false detections were associated with airplanes or earthquakes. By implementing additional steps such as a combined array classification and the localization of the events based on multiple signal classifications (MUSIC), we improved the classification results by reducing the number of identified events to 27. Only using the localization to remove false detections resulted in at least 15 % of false detections yet at a higher computational cost. Our results therefore show that dismissing false detections with a second array improves the overall classification accuracy. If a second avalanche monitoring array is in the vicinity, combing the results of both arrays will improve the classification results. In future experiments we want to reduce the distance between the arrays to some kilometers to improve the localization of avalanches and the combined array processing.

Acknowledgements. M.H. was supported by a grant of the Swiss National Science Foundation (200021_149329). We thank numerous colleagues from SLF for help with field work and maintaining the instrumentation.

Earth Surf. Dynam. Discuss., https://doi.org/10.5194/esurf-2018-36
Manuscript under review for journal Earth Surf. Dynam.
Discussion started: 3 May 2018

Competing interests. The authors declare that they have no conflict of interest.

References

Bessason, B., Eiriksson, G., Thorarinsson, O., Thorarinsson, A., and Einarsson, S.: Automatic detection of avalanches and debris flows by seismic methods, J. Glaciol., 53, 461–472, 2007.

Beyreuther, M., Hammer, C., Wassermann, J., Ohrnberger, M., and Megies, T.: Constructing a Hidden Markov Model based earthquake detector: application to induced seismicity, Geophys. J. Int., 189, 602–610, 2012.

Hammer, C., Beyreuther, M., and Ohrnberger, M.: A seismic-event spotting system for Volcano fast-response systems, B. Seismol. Soc. Am., 102, 948–960, 2012.

Hammer, C., Ohrnberger, M., and Fäh, D.: Classifying seismic waveforms from scratch: a case study in the alpine environment, Geophys. J. Int., 192, 425–439, 2013.

Hammer, C., Fäh, D., and Ohrnberger, M.: Automatic detection of wet-snow avalanche seismic signals, Nat. Hazards, 86, 601–618, https://doi.org/10.1007/s11069-016-2707-0, 2017.

Heck, M., Hammer, C., van Herwijnen, A., Schweizer, J., and Fäh, D.: Automatic detection of snow avalanches in continuous seismic data using hidden Markov models, Natural Hazards and Earth System Sciences, 18, 383–396, https://doi.org/10.5194/nhess-18-383-2018, 2018a.

Heck, M., Hobiger, M., van Herwijnen, A., Schweizer, J., and Fäh, D.: Localization of seismic events produced by avalanches using multiple signal classifications, Geophys. J. Int., under revision, 2018b.

Hobiger, M., Cornou, C., Bard, P.-Y., Le Bihan, N., and Imperatori, W.: Analysis of seismic waves crossing the Santa Clara Valley using the three-component MUSIQUE array algorithm, Geophys. J. Int., 207, 439–456, 2016.

Lacroix, P., Grasso, J.-R., Roulle, J., Giraud, G., Goetz, D., Morin, S., and Helmstetter, A.: Monitoring of snow avalanches using a seismic array: Location, speed estimation, and relationships to meteorological variables, J. Geophys. Res. Earth Surf, 117, F01 034, https://doi.org/10.1029/2011JF002106, 2012.

Leprettre, B., Navarre, J., and Taillefer, A.: First results from a pre-operational system for automatic detection and recognition of seismic signals associated with avalanches, J. Glaciol., 42, 352–363, 1996.

Marchetti, E., Ripepe, M., Ulivieri, G., and Kogelnig, A.: Infrasound array criteria for automatic detection and front velocity estimation of snow avalanches: towards a real-time early-warning system, Natural Hazards and Earth System Sciences, 15, 2545 – 2555, 2015.

McClung, D. and Schaerer, P. A.: The Avalanche Handbook, The Mountaineers Books, 2006.

Nishimura, K. and Izumi, K.: Seismic signals induced by snow avalanche flow, Nat. Hazards, 15, 89–100, 1997.

Ohrnberger, M.: Continuous automatic classification of seismic signals of volcanic origin at Mt. Merapi, Java, Indonesia, PhD. thesis, 2001.

Rost, S. and Thomas, C.: Array seismology: methods and application, Rev. Geophys., 40, 2.1–2.27, https://doi.org/10.1029/2000RG000100, 2002.

Rubin, M., Camp, T., van Herwijnen, A., and Schweizer, J.: Automatically detecting avalanche events in passive seismic data, IEEE International Conference on Machine Learning and Applications, 1, 13–20, 2012.

Schaerer, P. A. and Salway, A. A.: Seismic and impact-pressure monitoring of flowing avalanches, J. Glaciol., 26, 179–187, 1980.

Schmidt, R.: Multiple emitter location and signal parameter estimation, IEEE Trans. Antennas Propag., 34, 276–280, 1986.

Scott, E., Hayward, C., Kubichek, R., Hamann, J., Pierre, J., Comey, B., and Mendenhall, T.: Single and multiple sensor identification of avalanche-generated infrasound, Cold Reg. Sci. Technol., 47, 159–170, 2007.

Suriñach, E., Furdada, G., Sabot, F., Biescas, B., and Vilaplana, J.: On the characterization of seismic signals generated by snow avalanches for monitoring purposes, Ann. Glaciol., 32, 268–274, https://doi.org/10.3189/172756401781819634, 2001.

Suriñach, E., Vilajosana, I., Khazaradze, G., Biescas, B., Furdada, G., and Vilaplana, J.: Seismic detection and characterization of landslides and other mass movements, Nat. Hazards Earth Syst. Sci., 5, 791–798, 2005.

Thüring, T., Schoch, M., van Herwijnen, A., and Schweizer, J.: Robust snow avalanche detection using supervised machine learning with infrasonic sensor arrays, Cold Reg. Sci. Tech., 111, 60 – 66, 2015.

van Herwijnen, A. and Schweizer, J.: Seismic sensor array for monitoring an avalanche start zone: design, deployment and preliminary results, J. Glaciol., 57, 257–264, 2011a.

van Herwijnen, A. and Schweizer, J.: Monitoring avalanche activity using a seismic sensor, Cold Reg. Sci. Tech., 69, 165–176, 2011b.